Journal of the European Ceramic Society 16 (1996) 447–451

0955-2219(95)00119-0
0955-2219/96/$15.00

Localization of Oxygen Cathodic Reduction Zone at Lanthanum Manganite/Zirconia Interface

H. Lauret & A. Hammou

Laboratoire d'Ionique et d'Electrochimie des Solides de Grenoble (INPG-UJF), Associé au CNRS (URA 1213), ENSEEG, BP 75, 38402 Saint-Martin d'Hères Cédex, France

(Received 30 March 1995; revised version received 29 June 1995; accepted 14 July 1995)

Abstract

The electrochemical properties of $La_{0.45}Sr_{0.55}MnO_3$ have been studied under steady state polarization. The I–η curves have been obtained for three point electrodes with three different values of surface area of contact with the electrolyte, which is yttria-stabilized zirconia. The results obtained in the 0 to 160 mV overpotential range exhibit a current proportional to the length of the triple contact between the gas phase, the point electrode and the electrolyte. For higher cathodic overpotentials no direct proportionality between the current and the length of the triple contact nor the surface area of the contact between the electrode and the electrolyte was found. These facts were interpreted in terms of the progressive extension of the reaction zone from the triple contact line to the surface of the contact between the electrode and the electrolyte at conditions under which the electrode material exhibits mixed conductivity.

1 Introduction

Solid oxide fuel cells (SOFCs) are electrochemical devices in which much interest has been shown over recent decades. They are considered to have potential for electric power generation with high grade by-product heat. Furthermore, they are among the more desirable systems to reduce the environmental impact caused by fossil fuel consumption. SOFCs operate in the 800–1000°C temperature range and may be described by the following electrochemical chain: fuel gas, Ni-yttria-stabilized zirconia cermet anode / yttria-stabilized zirconia electrolyte / ceramic oxide cathode, air.

Perovskite-type oxides $La_{1-x}M_xMnO_3$ (M = Sr, Ca) have been selected as cathodes for their high electrical conductivity, their electrocatalytic properties for oxygen reduction and their thermal and chemical compatibility with the electrolyte material (yttria-stabilized zirconia). The major part of the power losses in these cells are due to the cathodic material. Therefore, many studies have been carried out to define the relationship between the cathodic overpotential, the oxygen reduction pathway and the intrinsic properties of these materials (e.g. microstructure, porosity). The oxygen reaction mechanism is still unknown.[1]

This work is an attempt to define where the oxygen reduction takes place (contact area or triple contact line) in order to modify the cathode microstructure accordingly. The material studied belongs to the strontium-doped lanthanum manganite (LSM) family. $La_{0.45}Sr_{0.55}MnO_3$ was chosen because of its high electrical conductivity among this family.[2] It is known that no solid state reaction involving the formation of new phases takes place at the manganite/zirconia interface at temperatures below 1100°C.[3]

2 Experimental Procedures

For the electrolyte, discs of yttria-stabilized zirconia (9% Y_2O_3) were prepared. Highly pure (>99·99%) Y_2O_3 and ZrO_2 reactant powders were mixed in appropriate amounts in ethanol, filtered, dried and sieved. The resulting powder were calcined at 900°C then compacted in the shape of a cylinder and pressed isostatically at 1500 bar. The sintering process was carried out in a reducing atmosphere at 1350°C for 2 h. During cooling the atmosphere was air. The sample had a density more than 95% of the theoretical density. The sample grain size was in the range 2–3 μm. The dense cylinder was cut into discs of 200 μm thickness.

The solid state reaction route was chosen for the Sr-doped lanthanum manganite sample preparation. The starting components were high purity $SrCO_3$, $MnCO_3$ and La_2O_3. The powders were dried at 80°C for several days to avoid hydration due to their hygroscopic nature. The appropriate

amounts of powders were ball-milled with ethanol in an agate mortar, then dried and compacted. The resulting cylinder was calcined at 1400°C for 4 h. During the increase of temperature carbonates were destroyed in a step between 850 and 1050°C; between these two temperatures the temperature increase was only 50°C h^{-1} instead of 100°C h^{-1} elsewhere. The sample was then ground and compacted into a cylinder in a uniaxial press at 200 bar and isostatically pressed at 3000 bar. The cylinder was sintered at 1400°C for 4 h. The grinding/compacting/sintering cycle was repeated twice.

After each cycle, X-ray measurements were performed to verify that no product other than the classical perovskite phase was present. The chemical analysis of the sample was performed by plasma emission spectroscopy. The results confirmed the expected composition. The cylinders obtained were dense enough (higher than 95% of the theoretical density) that machining into pin-shaped samples was feasible. Three point electrodes were prepared. Their ends were polished to obtain three different values of the surface area of contact with the electrolyte. This polishing operation was performed using a zirconia disc to avoid any chemical contamination.

We will call 'electrode material' the perovskite part of the 'electrode' which is, in fact, the perovskite material, the electrolyte and the surrounding atmosphere. The cell configuration is shown in Fig. 1. The cell was made in such a way that three working electrodes could be placed in the furnace and could be studied in parallel under the same conditions. They were arranged in an equilateral triangle. On the other side of the electrolyte the counter-electrode was annular and large enough to cover the area directly opposite the working electrodes. The reference electrode was central and its surface area was much smaller than that of the counter-electrode. The counter- and reference electrodes were made of a porous platinum coating (Degussa 308A). Platinum leads were cemented to the electrode materials with the same platinum paste. The cell temperature was controlled by a Pt/PtRh thermocouple placed close to the working electrode. The experiments were performed at 960°C in air.

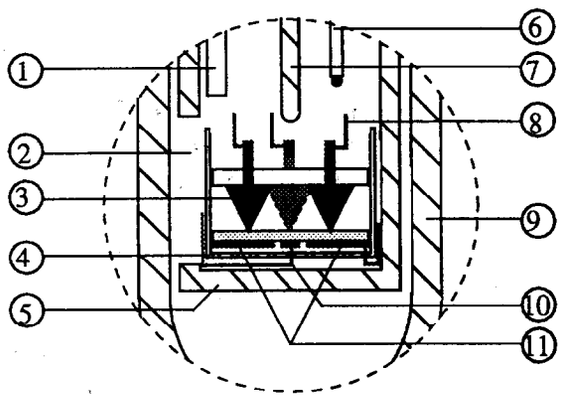

Fig. 1. Cell configuration. 1, Air entry tube; 2, alumina support; 3, electrode material; 4, alumina cup; 5, alumina sample holder tube; 6. thermocouple; 7, alumina tightening rod; 8, Pt wire; 9, alumina furnace tube; 10, reference electrode; 11, counter-electrode.

Potentiostatic and impedance spectroscopy measurements were carried out with a Tacussel Z-Computer potentiostat/impedance spectroscopy analyser, which allowed simultaneous polarization and impedance spectroscopy measurements in the frequency range 10^5–10^{-4} Hz. We limited the studied domain to 10^5–10^{-2} Hz. The ohmic drop in the cell was calculated using the high frequency intercept of the impedance diagram with the real axis. This high frequency intercept was corrected, if necessary, by taking into account the self-induction of the circuit (typically 10^{-6} H). The steady state polarization curves were drawn point by point for the three electrodes, one point a day in general, and an impedance spectroscopy measurement taken at each point.

3 Results and Discussion

3.1 Determination of surface contact area between electrode material and electrolyte

Two types of determination were made for evaluation of the surface contact area between the electrode material and the electrolyte. First, micrographs of the point electrode areas were taken before and after the experiment. We also took micrographs of the zirconia disc surface after the experiment. The electrode material left black spots of perovskite on the disc. The spot area allowed us to evaluate the minimum surface contact area.

The Newmann equation[4] was used as a second method for determination of the surface contact area. This equation is:

$$R_{el} = \frac{1}{4r\sigma_{el}}$$

where Rel is the electrolyte resistance determined by impedance spectroscopy and σ_{el} is the electrolyte conductivity determined with large electrodes

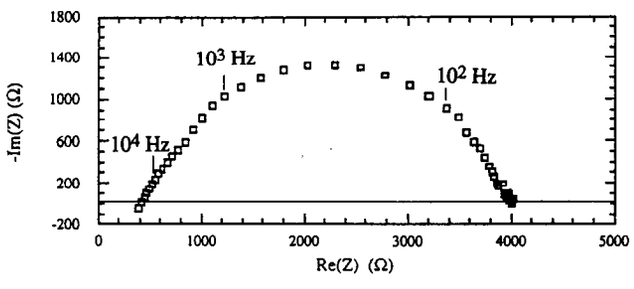

Fig. 2. Typical impedance spectra obtained on electrode C at 66 mV cathodic polarization.

Table 1. Geometrical parameters of the LSM/YSZ interface determined by microscopic observation

		Electrode A	*Electrode B*	*Electrode C*
Electrode observation*	S (cm^2)	$3{\cdot}8 \times 10^{-4}$	$5{\cdot}6 \times 10^{-4}$	$6{\cdot}1 \times 10^{-3}$
	L (cm)	0·07	0·14	0·28
Spot observation†	S (cm^2)	$2{\cdot}9A \times 10^{-3}$	$6{\cdot}85 \times 10^{-3}$	$2{\cdot}3 \times 10^{-3}$
	L (cm)	0·19	0·26	0·16
Newmann calculation	S (cm^2)	$2{\cdot}0 \times 10^{-3}$	$4{\cdot}4 \times 10^{-3}$	$1{\cdot}1 \times 10^{-3}$
	L (cm)	0·16	0·23	0·11

*Electrodes before use.
†Spot left by the electrode on ceramic electrolyte after use.

fully covering two sides of an electrolyte disc. In the present work, the value determined for the latter term was $9{\cdot}6 \times 10^{-2}$ S cm^{-1} at 960°C. r is the electrically determined average radius of the equivalent disc of the same area. From the r value we can deduce the surface contact area and the length of the contact if its shape is close to a disc. Table 1 shows the results of the microscopic observations and the electrical calculations. A typical impedance spectrum is shown in Fig. 2. From these results we see that there is no correlation between the observed contact area of the point electrodes before their use and the effective contact area. Actually, the electrode material may be badly placed so that the whole observed surface is not in contact with the electrolyte. This is the case for electrode C. Furthermore, the ceramic material may be slightly squashed in the case of the finest pin-shaped electrodes. This is the case for electrodes A and B.

Good agreement between the Newmann calculation and the observation of the spot left on the electrolyte by the electrode material was found. It is reasonable to give more credit to the Newmann formula than to the microscopic observations, because the latter enabled us to follow the values of the geometrical parameters during the experiment, even if these were changed accidentally.

3.2 Cathodic polarization results in the 0–160 mV domain

The steady state polarization curves are shown in Fig. 3. The currents are not normalized using the geometrical parameters. It can be seen, in particular, that the relative values of the current follow the geometrical parameters, the higher current being obtained with the point electrodes having the largest area, i.e. electrode B. In Fig. 4 these curves are normalized using the geometrical parameters. The normalization with respect to the optically determined parameters gives no conclusive results, as expected; the reliability of these parameters being low as mentioned before. On the other hand, the Newmann parameters give better results: a direct correlation between the oxygen reduction current and the contact perimeter is found with good accuracy.

Whereas the discrepancies between the three curves are within 4000 and 1000% in the case of the normalizations with respect to the optically determined perimeter and surface, respectively, the value is 260% in the case of the normalization with respect to the Newmann surface and only 33% with respect to the Newmann perimeter. So, we can confirm by means of the polarization and impedance measurements that the cathodic reduction process takes place through the contact perimeter, that is to say, the triple phase boundary between the gas, the electrode material and the electrolyte. The same conclusions have been drawn by other authors using similar materials ($La_{0.6}Ca_{0.4}MnO_3$)[5] or silver electrodes,[6] in experiments performed under zero polarization.

3.3 Cathodic polarization in the 160–500 mV domain

The steady state polarization curves in the whole range studied are shown in Fig. 5 for electrodes B and C. For this section, the parameters used are those deduced from the Newmann formula. In Fig. 6 it can be seen that neither normalization by the contact perimeter nor by the contact surface area is satisfactory. This result means that the

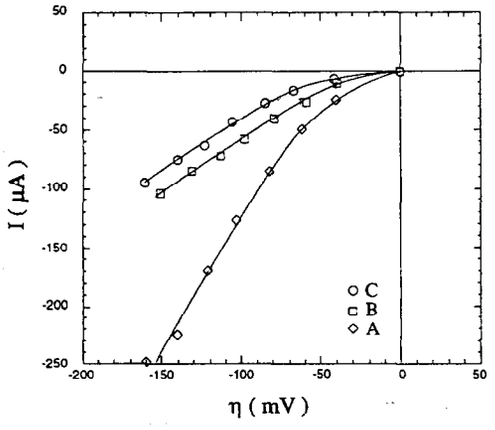

Fig. 3. Steady state polarization curves in the 0–160 mV cathodic polarization domain at 960°C on three point electrodes of $La_{0.45}Sr_{0.55}MnO_3$ (A, B and C) with different values of surface area of contact with the electrolyte.

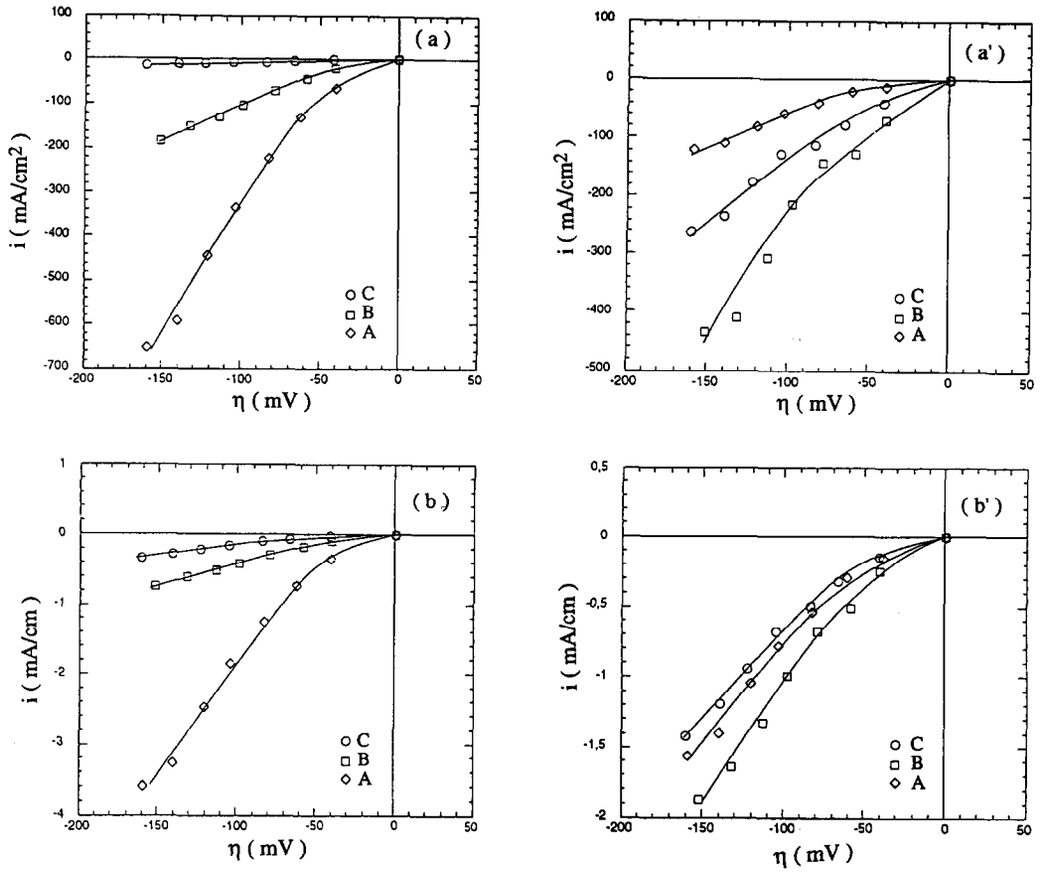

Fig. 4. Steady state polarization curves in the 0–160 mV cathodic polarization domain at 960°C on A, B and C. Currents are normalized by the geometrical parameters. (a) and (a') Optically determined length and surface area of the contact, respectively; (b) and (b') Newmann length and surface area of the contact, respectively.

reduction reaction process takes place neither at the triple phase boundary nor over the whole contact surface homogeneously. This behaviour may be explained as follows. Under high polarization (typically < –200 mV) the LSM system becomes a mixed conductor because of the formation of oxygen vacancies in the material.[7] The electrochemical reduction of oxygen may then occur at the lateral surface of the entire electrode material. The oxygen ions produced may diffuse through the electrode material from the electrode lateral surface to the electrode/electrolyte contact where they may enter the electrolyte. Thus, to the first pathway a second one is added.

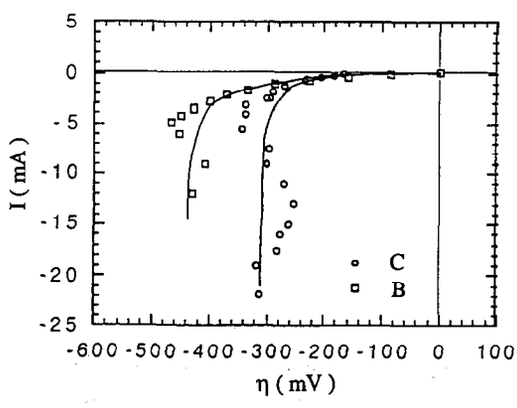

Fig. 5. Steady state polarization curves in the 0–500 mV cathodic polarization domain at 960°C on B and C.

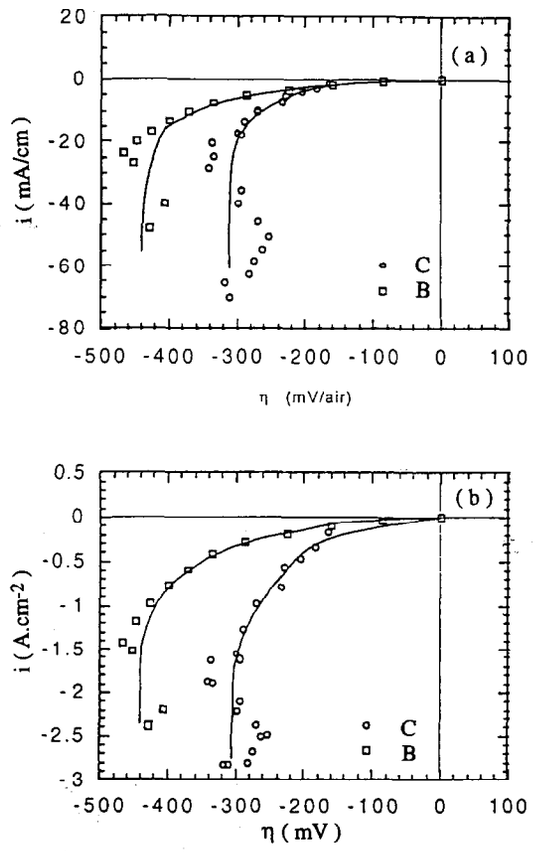

Fig. 6. Steady state polarization curves in the 0–500 mV cathodic polarization domain at 960°C on B and C. Currents are normalized by the geometrical parameters. (a) and (b') Newmann length and surface area of the contact, respectively.

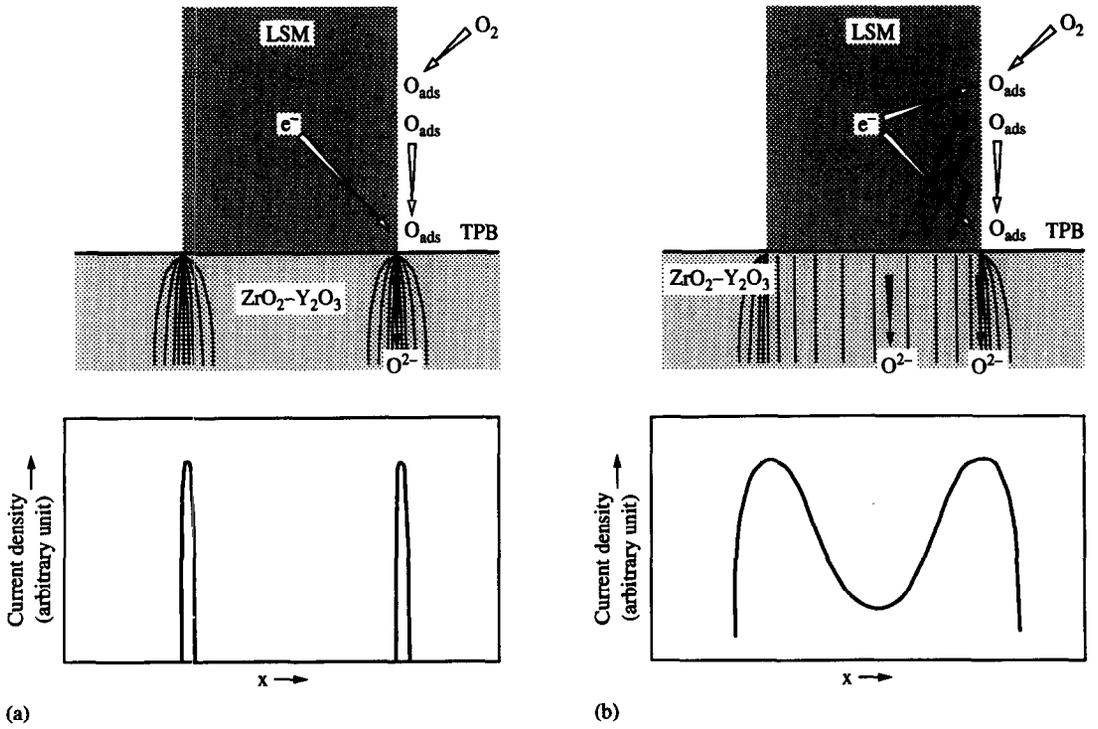

Fig. 7. Oxygen reduction pathways: (a) 0–160 mV cathodic polarization domain; (b) 160–500 mV cathodic polarization domain.

The possible outwards extension of the reaction zone from the triple phase boundary onto the free electrolyte surface by injection of electrons into the electrolyte, giving rise to another reaction pathway, cannot be neglected.[8] In this way, the reaction zone is extended inwards and outwards from the contact perimeter, giving rise to a current density distribution as shown in Fig. 7. So, the geometrically limiting surface is neither the perimeter nor a disc, but an annular zone around the contact perimeter in which the current is not necessarily homogeneous. As the three point electrodes have the same lateral surface area this cannot be the limiting surface.

4 Conclusions

In the present work, we have demonstrated the validity of the model describing the oxygen reduction on strontium-doped lanthanum manganite electrodes. At low polarization (typically > –200 mV at 960°C), the reduction takes place along the triple contact line between the gas phase, the electrode and the electrolyte materials. At higher polarization a second process is superimposed on the first. As the material becomes a mixed conductor in this domain, the appearance of oxygen vacancies in the electrode material allows the oxygen reduction to take place at the lateral surface of the electrode. This second process leads to the extension of the reaction pathway from the triple contact line to the entire contact surface between the electrode material and the electrolyte. Note that the data deduced from this second process would not be relevant to real fuel cell conditions, because of too high a cathodic overpotential. Further, it has to be emphasized that the geometrical factors used for this kind of study must be deduced from the impedance measurements by applying the Newmann formula.

References

1. Mogensen, M., *Proceedings of the 14th Symposium on Materials Science*, eds F. W. Poulsen, *et al.* Risø, 1993, pp. 117–35.
2. Lauret, H., Caignol, E. & Hammou, A., *Proceedings of the Second International Symposium on Solid Oxide Fuel Cells*, eds F. Grosz, P. Zegers, S. C. Singhal and H. Iwahara. Official Publications of the European Communities, Luxembourg, 1991, pp. 479–86.
3. Chen, C. C., Nasrallah, M. M. & Anderson, H. U., *Proceedings of the Third International Symposium on Solid Oxide Fuel Cells*, eds. S. C. Singhal and H. Iwahara. The Electrochemical Society, Inc., Pennington, NJ, 1993, pp. 598–612.
4. Newmann, J., *J. Electrochem. Soc.*, **113** (1966) 501–2.
5. Mizusaki, J., Tagawa, T., Tsuneyoshi, K. & Sawata, A, *J. Electrochem. Soc.*, **138** (1991) 1867–73.
6. Kleitz, M., Dessemond, L., Kloidt, T. & Steil, M. C., *Proceedings of the Fourth International Symposium on Solid Oxide Fuel Cells*, eds M. Dokiya, O. Yamamoto, H. Tagawa and S. C. Singhal. The Electrochemical Society, Inc., Pennington, NJ, 1995, pp. 527–36.
7. Hammouche, A., Siebert, E., Hammou, A., Kleitz, M. & Caneiro, A., *J. Electrochem. Soc.*, **138** (1991) 1212–16.
8. Kleitz, M., PhD Thesis, Université de Grenoble, France, 1968.